



## Localised opto-thermal response of nematic liquid crystal to laser light

U. Jagodič, A.V. Ryzhkova & I. Muševič

To cite this article: U. Jagodič, A.V. Ryzhkova & I. Muševič (2019) Localised opto-thermal response of nematic liquid crystal to laser light, *Liquid Crystals*, 46:7, 1117-1126, DOI: [10.1080/02678292.2018.1557270](https://doi.org/10.1080/02678292.2018.1557270)

To link to this article: <https://doi.org/10.1080/02678292.2018.1557270>



Published online: 17 Dec 2018.



Submit your article to this journal [↗](#)



Article views: 106



View related articles [↗](#)



View Crossmark data [↗](#)



## Localised opto-thermal response of nematic liquid crystal to laser light

U. Jagodič<sup>a</sup>, A.V. Ryzhkova<sup>a</sup> and I. Muševič<sup>a,b</sup>

<sup>a</sup>Department of Condensed Matter Physics, J. Stefan Institute, Ljubljana, Slovenia; <sup>b</sup>Faculty of Mathematics and Physics, University of Ljubljana, Ljubljana, Slovenia

### ABSTRACT

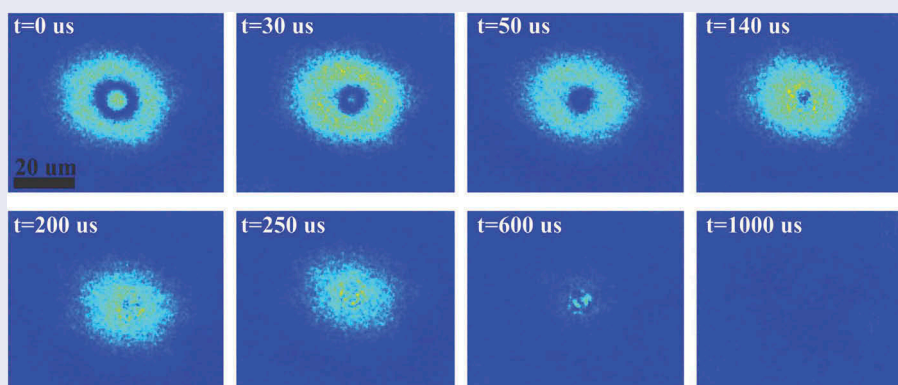
We report on the thermal response of a thin nematic liquid crystal layer to a strong laser pulse, which is partially absorbed by the Indium Tin Oxide electrodes of the measuring LC cell. We measure local increase and temperature profile of the heated region and we measure the time response of the birefringence of this nematic layer. It is found that local increase of the temperature due to absorption of a 90 Mw laser light of 10 MS duration can easily exceed 100°C and depends on the localisation and focusing of the laser beam. Local thermal response of the heated nematic cell is measured by monitoring the time dependence of birefringence during the cooling and we found that nematic layer can be cooled down at an extremely fast rate of 10000 K/s. Optical retardation of ~200 nm can be switched in ~100 μs by laser pulse absorption and heating/cooling.

### ARTICLE HISTORY

Received 9 October 2018  
Accepted 5 December 2018

### KEYWORDS

Opto-thermal effect; liquid crystals; thermal properties; Kibble-Zurek mechanism



## 1. Introduction

Optical trapping of particles [1] in the nematic liquid crystals [2–12] has opened an exciting research direction which demonstrated assembly of artificial colloidal structures for novel photonic applications. It has been demonstrated that the physics of optical trapping by means of a strongly focused laser light in liquid crystals is significantly different compared to optical trapping in isotropic fluids. Several trapping mechanisms have been demonstrated, and among them the opto-thermal trapping has proved to be very general and allows for trapping and manipulation of arbitrary objects in liquid crystals [13].

Thermal response of a nematic liquid crystal is nowadays used for manipulation of the colloidal particles dispersed in the liquid crystal by means of the optical tweezers. By using a strong laser light of the tweezers, significant portion of the laser power can be absorbed in

the liquid crystal directly or indirectly, thereby increasing the local temperature of the liquid crystal during the illumination [13]. Local increase of the temperature results in local decrease of the degree of nematic order parameter  $S$ , which creates strong gradients of the order and gives rise to significant structural forces that are used to trap and manipulate the particles in the NLC.

Local heating of the NLC by laser light can be realised in several ways. If the liquid crystal is made absorbing either by dispersing dye molecules or metal nano-particles in it, the direct absorption of laser light in these objects results in efficient and very localised heating of the liquid crystal. This direct heating has in fact been used widely in nonlinear optical studies, demonstrating interesting all-optical effects in dye-doped liquid crystals [14–17]. Light absorption in azodye-doped liquid crystals is used to induce transitions in the optical transmission for smart windows and other applications [18,19].

Indirect heating of the liquid crystal by light is made possible by light absorption in the thin ITO layer, deposited on the inner surfaces of the cell containing the liquid crystal. This way of indirect heating is commonly used for colloidal trapping and manipulation by the strong light of the optical tweezers and the mechanism was described and used in a large number of experiments [7,10,11,13]. It is interesting to note that this indirect heating by light was used for successful in-situ patterning of the nematic liquid crystal-ITO interface in an already assembled cell [20]. The mechanism relies on scanning a strong and focused laser spot along the alignment layer of the LC cell. Laser-assisted local melting of the liquid crystals creates a moving isotropic-nematic interface, which determines the surface alignment after the scanning. In principle this method could be used for thermal patterning of different alignment layers in already assembled LC devices.

In spite of the wide spread use of the optical tweezers for colloidal manipulation and tweezing by opto-thermal effect, little is known about the real parameters of this effect in LC cells. For example, it is not known what is the local temperature in the centre of the illuminating spot of the laser tweezers or what is the time response of a thin LC layer subjected to this opto-thermal effect. Jagemalm et al. [21] reported experiments on opto-thermal reorientation of nematics by heating the LC with a powerful laser. They determined the local temperature of the heated LC cell, but the opto-thermal dynamics and precise determination of the energy required to drive the NLC reorientation was not fully addressed because of a different scope of the paper.

To illuminate these open questions we report on the measurements of local temperature and temperature profile of a nematic liquid layer of a thickness between 2.5 and 17.5  $\mu\text{m}$  when a light pulse of 10 ms duration is absorbed by the 50 nm thick ITO layer deposited on the 170  $\mu\text{m}$  thin glass of the planar nematic cell. We also report the time dependence of this local temperature after the heating light is switched off, which is measured by monitoring the time dependence of the birefringence of the cell. Surprisingly, the cooling rates are extremely high and up to 10,000 K/s. This sub-millisecond switching dynamics opens up possibilities to use local laser heating and subsequent cooling in experiments that are testing the Kibble-Zurek mechanism of defect production in liquid crystals [22,23].

## 2. Materials and experimental set-up

We have used three different nematic liquid crystals in the experiments, which have very different clearing points. 5CB has the nematic to isotropic phase transition at  $T_o = 35.5^\circ\text{C}$ , E18 has the nematic to isotropic phase

transition at  $T_o = 60^\circ\text{C}$  and MLC 13,300 at  $T_o = 90^\circ\text{C}$ . Several cells were made of flat glass of thickness 170  $\mu\text{m}$  (purchased from Diamond Coatings) with two different thickness, 2.5  $\mu\text{m}$  and 17.5  $\mu\text{m}$ . The spacing was provided by glass spacers and the thickness of empty cells was determined using optical spectro-photometer (Ocean Optics USB2000). The glass slides have a 50 nm thin Indium Tin Oxide (ITO) coating, which serves as a light absorbing medium, thus providing a very efficient and localised heating of the NLC layer in good thermal contact with the ITO. The surfaces of the ITO coated glass were coated with a 30nm layer of polyimide (PI 2555 – Nissan Chemicals) which was rubbed with a velvet cloth to provide excellent planar and homogeneous alignment of the NLCs. In some cases, the ITO surface was coated by silane monolayer (DMOAP) to provide excellent homeotropic alignment. Because of a rather thick layer of ITO, the assembled glass cells showed rather strong light absorption, with an average transmission in the visible range of around  $\sim 75\%$ . This provides dissipation of approximately one quarter of the optical power in the two ITO layers. Glass cells were infiltrated with NLC by capillary action.

The set-up for studying the opto-thermal response of NLCs to strong laser pulses is presented in Figure 1. It was built around an inverted optical microscope (Nikon Eclipse TiDH) equipped with 100 x magnification objective (Nikon Plan Apo) with Numerical Aperture  $NA = 1.4$  and working distance of 170  $\mu\text{m}$ . The objective was put in good optical contact with the glass of the measuring cells thus eliminating multiple reflections at surfaces. The source of the laser light used for heating the ITO of the sample cell was a CW diode laser with  $\lambda = 532\text{nm}$  (MGL-III-200mW – Chanchung New Industries Optoelectronics Technology Co., Ltd.) with variable optical output power in the range from 1 mW to 200 mW. The CW laser could be triggered by external Digital Pulse Delay Generator (DG645 – Stanford Research Systems) to turn the laser on at predefined time and turn it off at another predefined time. Typically the time interval when the laser was turned-on was 10 ms, which was long-enough to reach the equilibrium temperature of the heated region of the cell. Such a short laser pulse provided enough energy to heat most of the NLCs used in our experiments into the isotropic phase. All experiments were performed at room temperature of  $21^\circ\text{C}$ .

The beam of the heating laser was expanded using the Gaussian type expander with two lenses of focal lengths  $L1 = 80\text{mm}$  and  $L2 = -25\text{mm}$ . The distance between the lenses could be precisely adjusted to a desired value by a precision translator, where one of the lenses was mounted. This beam expander allowed us to control the diameter of the illuminating (i.e. heating) spot on the

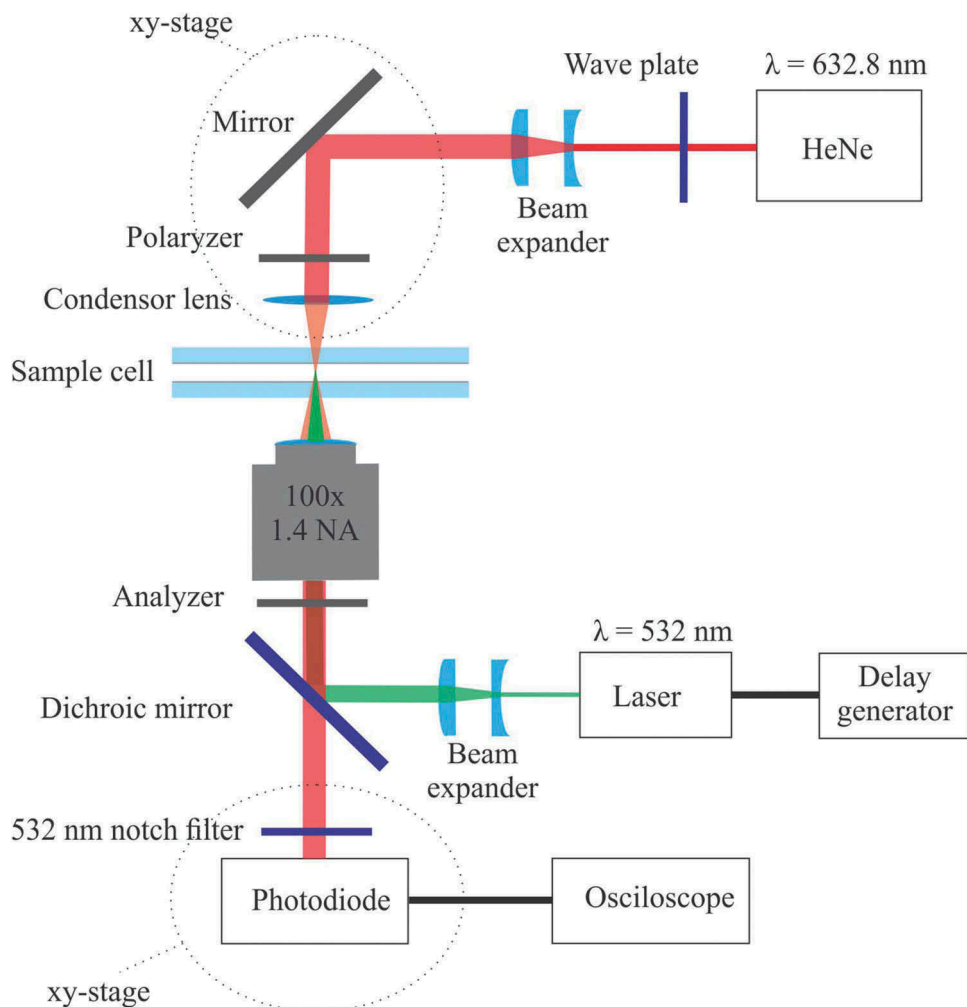


**Figure 1.** (Colour online) Experimental set-up for laser heating of the LC and measuring the time-dependence of the birefringence during rapid cooling of the LC.

front ITO layer. It could be adjusted in the range between  $1\ \mu\text{m}$  to  $70\ \mu\text{m}$ . The size of the heating spot was measured simply by observing the green illuminated spot on the ITO through the microscope.

In addition to measuring the time-dependence of the birefringence after the heating laser was switched-off, we used stroboscopic imaging to observe the texture of the heated region at a predefined delay time after the heating was switched-off. The part of the set-up which was used to image the LC texture during the fast temperature quench was built around the same microscope as the set-up for transmission measurement and is shown in [Figure 2](#). After the heating laser is switched off (with a fall-time of  $\sim 6\ \mu\text{s}$ ), individual images are taken after some preset delay time practically instantaneously, i.e. in a 20 ns illumination time, which makes the individual images extremely sharp. This strong optical flash is generated from a Nd:Yag pulsed laser (Ekspla PL2250), which is triggered by our pulse delay generator and produces 30 pulses with a peak pulse energy of up to

50 mJ. This coherent light is then focused to a glass cuvette filled with laser fluorescent dye solution (Rhodamine 6G) in ethanol. Each coherent laser pulse of 30 ps duration creates a 20 ns fluorescent pulse from Rhodamine 6G solution. A part of this light is very efficiently collected by a miniature optical system that shall be described elsewhere [24]. One should note that the fluorescent light is incoherent and is therefore suitable for high quality optical imaging. It is collected with an efficiency of nearly  $\sim 20\%$  into the fibre coupler (PAFSMA7A) by using a lens with 10 mm focal distance and transported to the microscope. Here we use a 15 mm lens to illuminate homogeneously the viewing field of the LC sample, placed in the plane of imaging.

The images are taken by using a 100 x magnification objective (Nikon Plan Apo) with a high Numerical Aperture (NA) of 1.4 and working distance of  $130\ \mu\text{m}$ . The objective and the glass of the cell containing the nematic LC are indexed matched. We use s-Cmos camera (Andor Neo) equipped with cooling system to

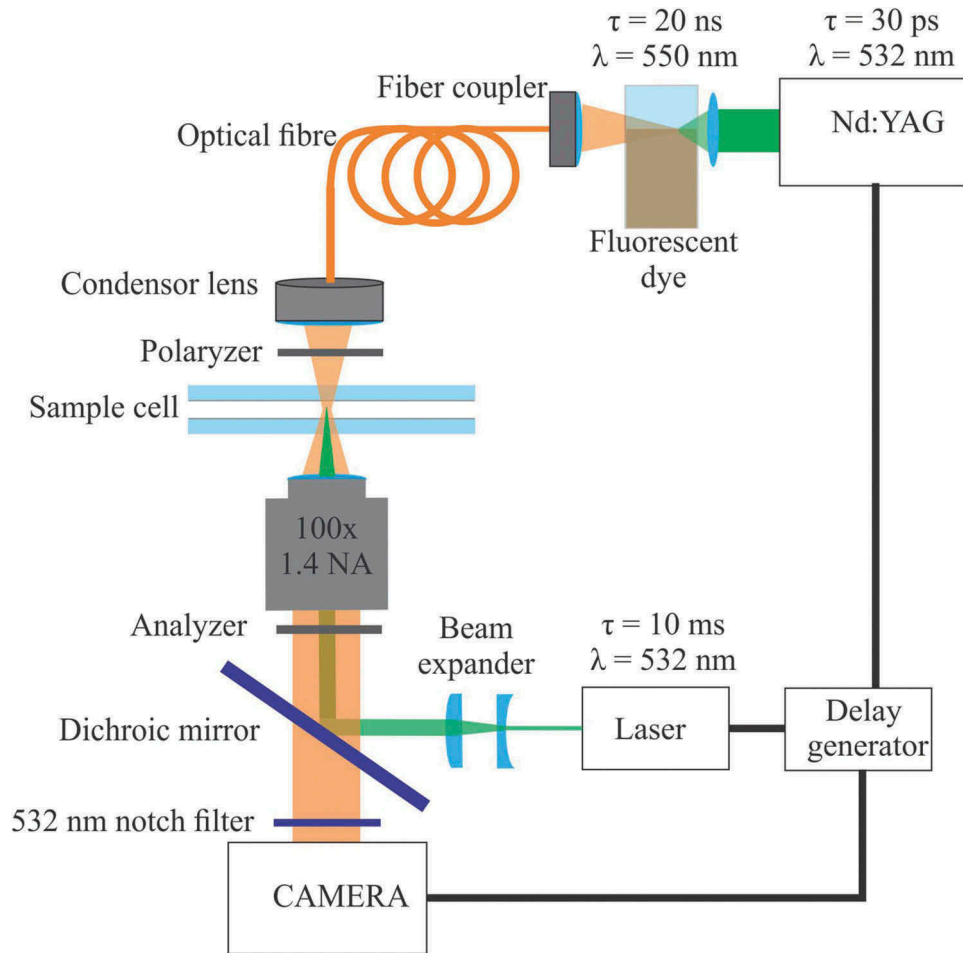


**Figure 2.** (Colour online) Experimental set-up for stroboscopic imaging of nematic texture after switching-off the heating laser. The system takes images at a predefined delay with a 20 duration of the ‘flash’ light.

reduce the thermal noise of the imaging chip. The camera is operating in the external triggering mode. The image acquisition of the camera is enabled during the 20  $\mu$ s time interval. In another words, all light which hits the imaging chip within the time interval of 20  $\mu$ s creates the image. Most of the time the camera receives no light, except at the 20 ns flash which illuminates the at-that-time-formed structure in the sample. In this way, we obtain extremely sharp images, with no blur due to the dynamics of the structure. Moreover, long active times of the camera, when the shutter is open, provides smooth operation of the electronic hardware for storing and transferring the data. The size of each pixel of the camera is 6.5  $\mu$ m which corresponds to 65 nm in the imaging plane using 100 x objective. The camera has 2560  $\times$  2180 pixels.

### 3. Experiments and results

We are interested in the time-dependence of the local temperature of the heated spot when the light is

switched off. To this aim we measure the time-dependence of the cell transmission between crossed polarisers for monochromatic light of another He-Ne laser (Uniphase 10 mW), as shown in Figure 1. We used crossed polarisers and the cell was rotated with respect to polarisation direction at 45°. In this configuration the transmission of the **nonpolarised incoming light**  $I_o$  of the cell is [25]

$$I = \frac{I_o}{2} \cdot \sin^2(2\phi) \cdot \sin^2 \left[ \frac{\pi \Delta n d}{\lambda} \right] \quad (1)$$

Here the angle  $\Phi$  is the angle between the nematic director in the planar cell and the polariser (hence  $\Phi = 45^\circ$ ,  $\Delta n$  is the birefringence of the liquid crystal,  $d$  is the thickness of the LC layer and  $\lambda$  is the wavelength of the measuring light (632.8 nm). Now, when the measured spot is cooling down, the birefringence of the NLC is changing with the instantaneous temperature, which means that the birefringence is a function of time,  $\Delta n(T(t))$ . Provided we know the temperature

dependence of  $\Delta n(T)$ , and we measure the time-dependence of the transmitted light between crossed polarisers,  $I(t)$ , we can calculate the time dependence of the local temperature  $T(t)$ . If we consider that the temperature dependence of the birefringence shows a power-law behaviour,  $n(T) = A \cdot \left(1 - \frac{T}{T_c}\right)^\alpha$ , the local temperature  $T$  at a given time  $t$  shall follow:

$$T(t) = T_c \cdot \left(1 - \left(\left(k\pi - \arcsin \sqrt{\frac{2I}{I_c}}\right) \cdot \frac{\lambda}{d\pi}\right)^{\frac{1}{\alpha}} \frac{1}{A}\right) \quad (2)$$

Here  $k$  describes the retardation order. We first measured the temperature dependence of both refractive indices of E18 using the Abbe-type refractometer equipped with a custom heating stage. Their temperature dependencies and the temperature dependence of the birefringence are shown in Figure 3. The temperature dependence of the birefringence could well be fitted to a power law  $\Delta n(T) = A \cdot \left(1 - \frac{T}{T_c}\right)^\alpha$  with the best-fit parameters  $\alpha = 0.21$ ,  $A = 0.25$  and  $T_c = 60.1^\circ\text{C}$ .

In the next step, we measured the local ‘stationary’ temperature, as induced by various power of the heating laser light and different diameter of the laser beam spot at the cell by simply taking the photographs under the microscope. The dependence of the diameter  $2r$  of the isotropic island of three different NLCs (5CB, E18 and MLC 13,300) as a function of the CW applied laser power is shown in Figure 4(a). The diameter  $2r$  starts to grow from zero at some value of the laser power, which means that for this laser power the temperature in the centre of the heated region just reaches the clearing point of that particular NLC. For example, the clearing point of E18 is at  $60^\circ\text{C}$ , and this is obtained at the laser power of 22 mW. Figure 4(b) shows the

temperature at the centre of the heating laser spot illuminating the ITO as a function of the CW power of the heating laser, as deduced from three different NLCs presented in Figure 4(a).

The diameter of the heating beam was measured by taking another cell with fluorescent labelled NLC and illuminating it with the heating laser. From the intensity image of the fluorescent emission area, the diameter of the Gaussian heating beam could be determined. The diameter of the beam is important for the in-plane temperature gradient in the cell, because the surface distribution of the dissipated heat strongly depends on this diameter. For very localised and strongly focused heating beam we expect very high temperature in the centre of the heated spot and rather narrow distribution of the temperature within the plane of the cell (i.e. the  $x - y$  plane). When the beam is made broader, the same amount of heat is dissipated over larger surface area and the expected temperature in the centre of the heated area should be lower, with a broader temperature distribution in the  $x - y$  plane.

The measurements of the diameter of the isotropic island of a chosen NLC allows us to determine the temperature in the centre of the illuminated area for any value of the heating power. For example, we present in Figure 5 the distribution of temperature at 90 mW heating power, as calculated from data points in Figure 4(a). By taking a Gaussian fit one can determine the temperature in the centre of the heating area, illuminated by the heating laser. Note that this value of  $102^\circ\text{C}$  is in close agreement with extrapolated temperature of  $103^\circ\text{C}$  from Figure 4(b).

After determining the ‘stationary’ temperature at the centre of the illuminated area of the NLC cell and its in-plane distribution, we measured the time

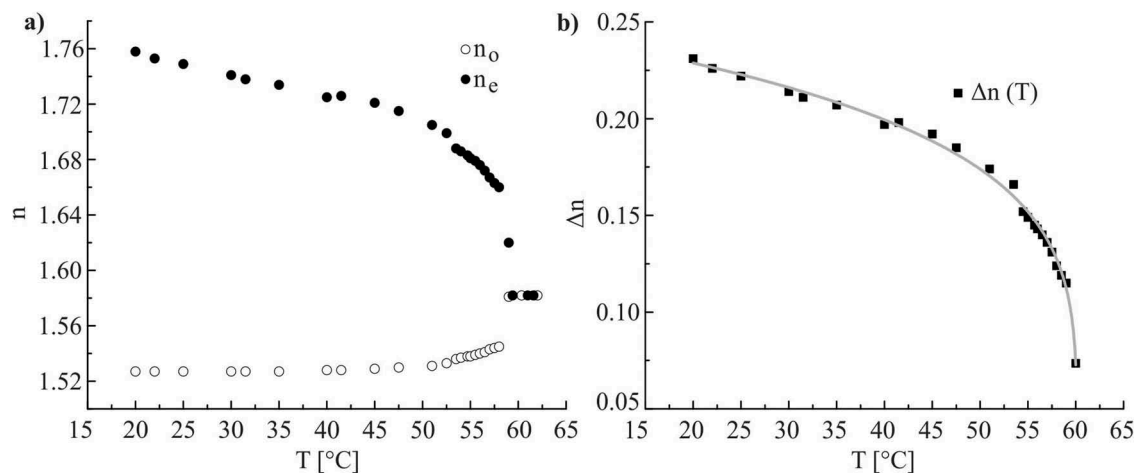


**Figure 3.** (a) Temperature dependence of the ordinary and extraordinary refractive indices for E18. (b) Temperature dependence of the birefringence of E18, fitted to power law  $\Delta n(T) = A \cdot \left(1 - \frac{T}{T_c}\right)^\alpha$  with the best-fit parameters  $\alpha = 0.21$ ,  $A = 0.25$  and  $T_c = 60.1^\circ\text{C}$ .

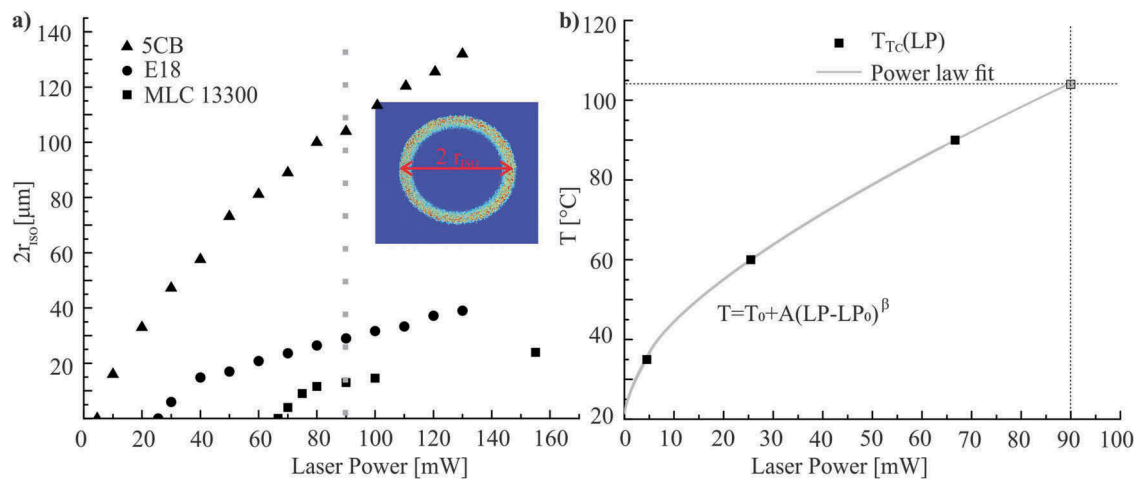


**Figure 4.** (Colour online) (a) The dependence of the diameter  $2r_{iso}$  the isotropic island of three different NLCs (5CB, E18 and MLC 13,300) as a function of the CW applied laser power at 532 nm. The inset shows an example of the isotropic island of 5CB in a 2.5  $\mu\text{m}$  thick cell with ITO. The diameter of the illuminated area was 95  $\mu\text{m}$ . Note that at the power level where the diameter of the isotropic island is equal to zero, the temperature in the centre is equal to the clearing point of that particular NLC. (b) The temperature at the centre of the heating laser spot illuminating the ITO as a function of the CW power of the heating laser. This was deduced from the graphs presented in (a). Note that the heating laser was applied only during 10 illumination time. The solid line is the best power-law fit of the form  $T = T_0 + A(LP - LP_0)^\beta$ , with  $T_0 = 21.8$ ,  $A = 5.3$ ,  $LP_0 = 0.006$  and  $\beta = 0.61$ .

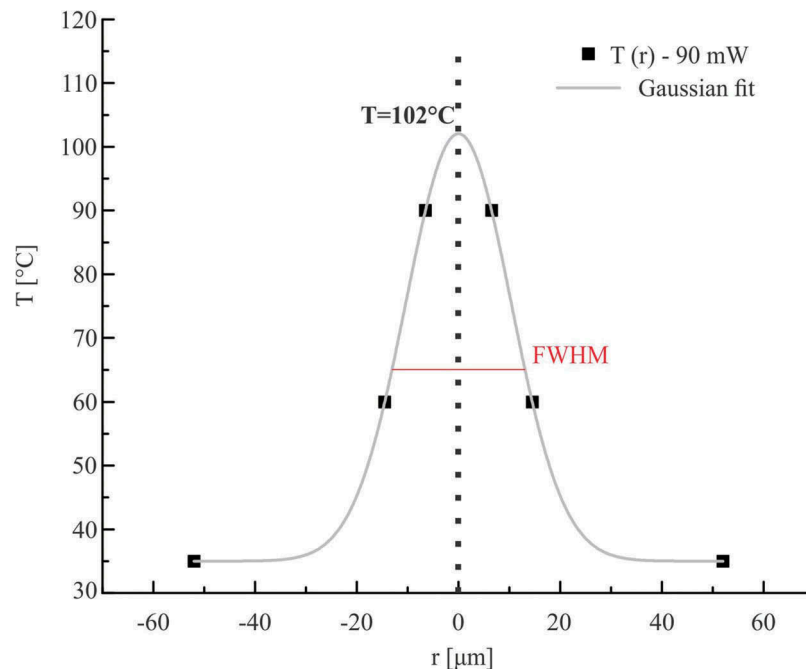


**Figure 5.** (Colour online) The distribution of temperature within the plane of the 2.5  $\mu\text{m}$  thin cell filled with a NLC for the heating power of 90 mW, applied for 10 ms. The points are taken from panel (a) of Figure 3. The solid line is the Gaussian fit to the experimental points, which gives us the temperature of  $102^\circ\text{C}$  in the centre of the illuminated area.

dependence of the temperature in the centre of the illuminated cell after the heating laser was switched-off. The measurement was performed on the 2.5  $\mu\text{m}$  thin cell of E18 and the CW power of the heating laser was set to 22 mW, i.e. just below the clearing temperature of E18. We estimate that the starting temperature

was around  $59^\circ\text{C}$ . The measured time-dependence of the transmitted intensity  $I(t)$  is shown in Figure 6.

Using the data in Figure 6 and Equation (2) we can reconstruct the time-dependence of the temperature  $T(t)$  in the centre of the cell, which is presented in Figure 7. The result is rather surprising, as we see

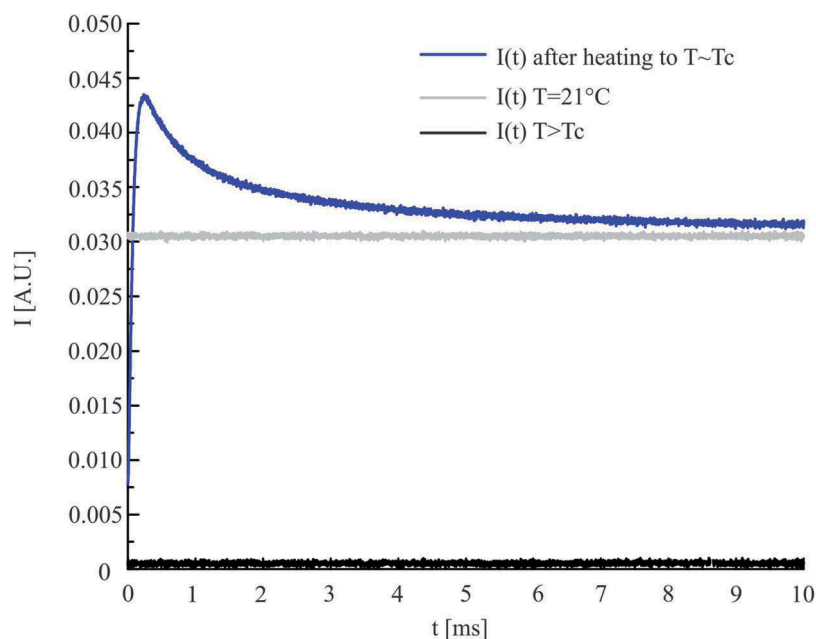


**Figure 6.** (Colour online) Time dependence of the laser light transmission of a 2.5  $\mu\text{m}$  planar nematic cell of E18 between crossed polarisers set at  $45^\circ$  (blue curve). The starting temperature at  $t = 0$  is  $\sim 59^\circ\text{C}$ , just below the clearing point. The grey line represents the signal transmission at room temperature and the black line the transmission in the isotropic phase. Note that the polarisers are crossed.

that the NLC layer cools-down very rapidly. The cooling rates are around 40 K in 1 ms, which corresponds to 40.000 K/s. This is enormously fast cooling rate and is primarily due to good thermal conduction of the 50 thin ITO layer. The best fit to this time dependence of the temperature is a two-exponential

fit with two different time constants and amplitudes. This two-time constant decay of temperature is most probably related to heat diffusion in two different directions, i.e. perpendicular to the interface and along the interface. The faster component of cooling has the time constant of  $\sim 90\mu\text{s}$  and is due to heat

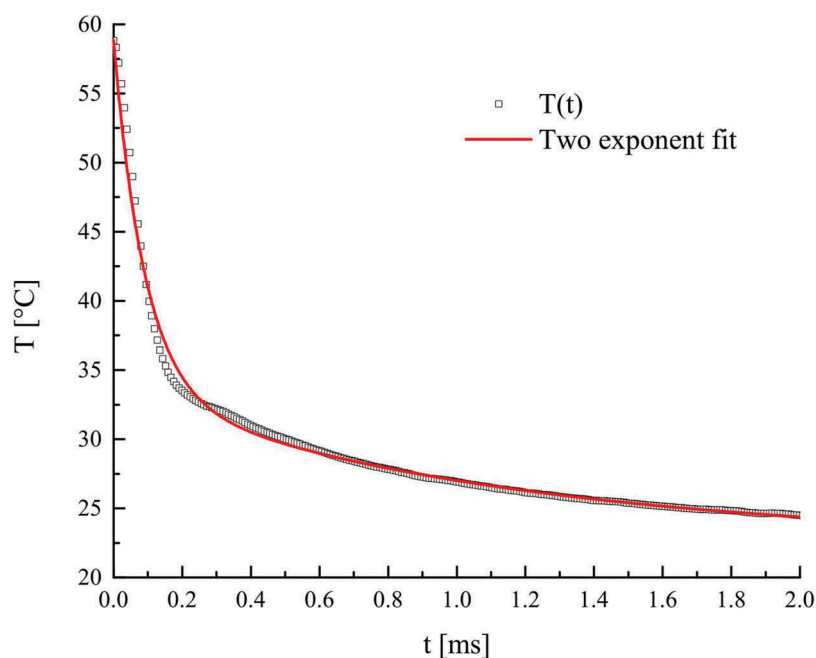


**Figure 7.** (Colour online) Time dependence of the temperature in the centre of 2.5 $\mu\text{m}$  planar nematic cell of E18 between crossed polarisers set at  $45^\circ$ . The starting temperature at  $t = 0$  is  $\sim 59^\circ\text{C}$ . The red solid line is the best two-exponential fit with time constants  $\tau_1 = 0.09$  ms and  $\tau_2 = 1.51$  ms. The signal with  $\tau_1$  has the amplitude of 10K, whereas the other signal has the amplitude of 30K.

flow across the ITO layer and into the glass substrate of the cell. The slower heat diffusion with more than an order of magnitude larger time constant of  $\sim 1.5$  ms is due to along-the-ITO heat flow. These results are also confirmed with our off-line simulations of heat flow using the COMSOL software.

In addition to measurements of birefringence during rapid cooling of the NLC we performed also stroboscopic imaging of birefringent pattern of the heated region with preselected delay times. Figure 8(a) shows selected snapshots of a  $17.5\ \mu\text{m}$  thick planar cell of E18 with 50 nm ITO coating. The laser power was set at 20 mW CW and the optical heating pulse was applied for 10ms. After switching-off the heating laser, an image of the heated region of the E18 was taken between crossed polarisers at pre-set delay times. The sequence of images in Figure 8(a) shows the

birefringence pattern of circular shape that shrinks in the course of time due to the heat flow and cooling down. There are approximately two fringes in the centre of the first image at zero delay (i.e. immediately after switching-off the heating light). In less than 1 ms the birefringent pattern completely fades away. Figure 8(b) shows the time-sequence of the intensity cross sections through the centre of the heated region. The picture clearly shows how the fringes shrink and disappear in a time of  $\sim 600\ \mu\text{s}$ .

From the sequence of images shown in Figure 8(b) one can reconstruct the time-dependence of the optical retardation (by following the positions of minima and maxima) and by knowing the temperature dependence of the birefringence (Figure 3(b)) one is able to reconstruct the time-dependence of the temperature at one particular point. on the image. Figure 9 shows

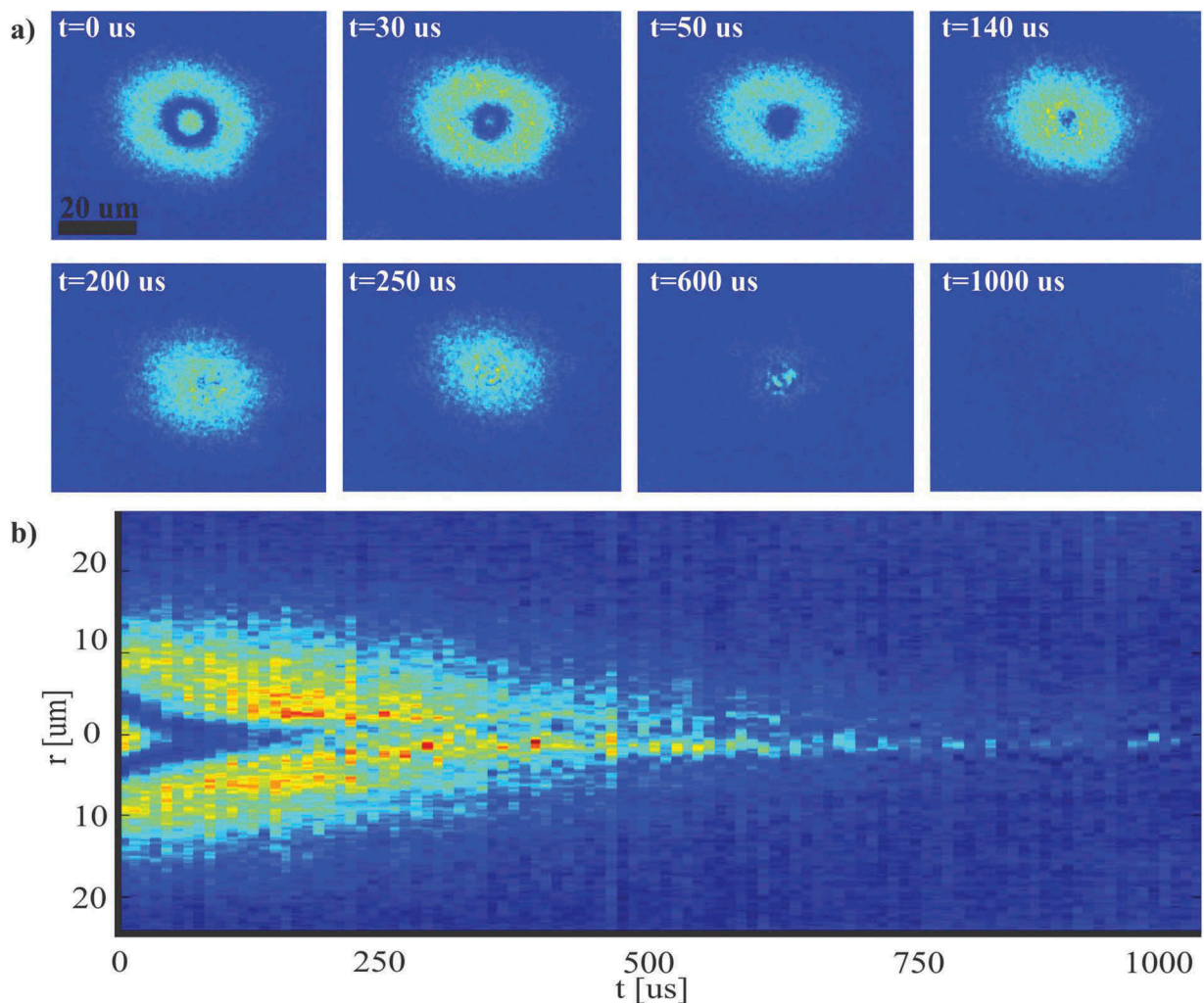


**Figure 8.** (Colour online) (a) Sequence of stroboscopic images of a  $17.5\ \mu\text{m}$  thick planar cell of E18 taken between crossed polarisers set at  $45^\circ$  at different delay times after switching-off the heating laser. The light intensity pattern is due to different local temperature and therefore different birefringence of the E18 LC. (b) The set of light intensity cross sections taken for the frames shown in (a) and also other frames at different delay times. The cross sections are taken through the centre of the heated region as illustrated in the first frame taken at zero delay.

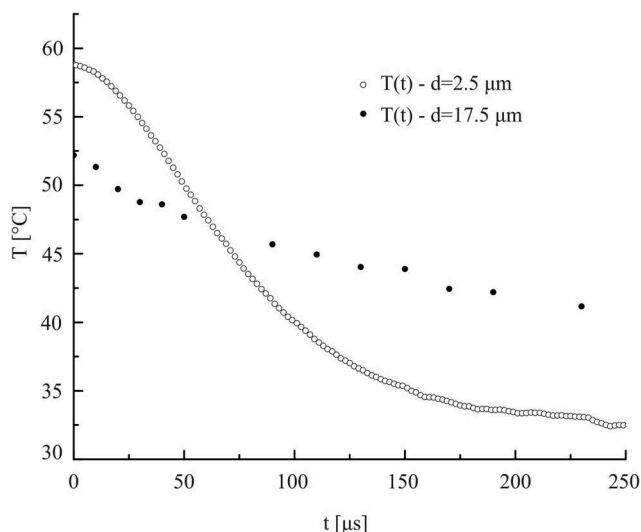


**Figure 9.** Time-dependence of the temperature in the central spot of the laser-heated region, shown in the sequence of images in Figure 8(a,b). Open circles are data reconstructed from the measurements of transmitted light intensity between crossed polarisers for the 2.5  $\mu\text{m}$  cell (taken from Figure 7). Full circles are values of temperature, as reconstructed from the sequence of delayed images in Figure 8(a,b), taken on 17.5  $\mu\text{m}$  cell filled with E18.

reconstructed time-dependence of the temperature in the centre of the heated region in 17.5  $\mu\text{m}$  thick cell of E18 for the first 250  $\mu\text{s}$  after switching-off the heating light. For comparison, thermal response of a 2.5  $\mu\text{m}$  thin cell of E18 is also presented, which shows significantly shorter decay time.

#### 4. Discussion

This work sheds new light on the physics of optothermal phenomena that has been used in many laser tweezers studies of nematic colloids in the past 15 years. In those studies, strong and focused light of the laser tweezers was used to locally melt the LC into the isotropic phase or raise the local temperature up to very close to the clearing point. Due to the softness of the LC and modified elasticity, it was possible to influence the structure of topological defects and induce their rewiring [10,11]. In another study, Mirri et al. [20] have used strong absorption of laser light in ITO to modify the surface alignment and literally “draw” alignment patterns of the LC *in situ*. While the optothermal method was found to be very useful in these topological studies, little was known about thermal and temporal properties of the method.

Our results reveal two key parameters of the optothermal effect in LCs. First, local temperature in the

centre of the heating laser spot can be extremely high and can easily exceed 100°C for moderate illumination laser power of 100 mW and illumination time of 10 ms. Second, thermal time constants of a 2–5  $\mu\text{m}$  thick LC cell with ITO are extremely short and are well below 1 ms. For example, a 2.5  $\mu\text{m}$  thin layer of a NLC can be cooled for 30–50°C in a time of  $\sim 500$   $\mu\text{s}$ . In another words, cooling rates of thin ITO cells allow for quenching rates of the order of 10000K/s. Such a rapid cooling could find interesting applications in non-equilibrium dynamical experiments, such as for example Kibble-Zurek experiments. Here the phase transition point is rapidly traversed at a fast and pre-determined quench rate, and the system develops after crossing the phase transition point a multitude of topological defects that are subject to growth and coalescence. So far, these kind of experiments were not able to control and measure the temperature during the fast quench, which is now demonstrated in full detail. We are confident that this work shall stimulate further research in non-equilibrium dynamics of soft matter phase transitions.

On the other hand, one is wondering if this optothermal effect, which is quite fast, could be used in some sort of display application. Because of the thermal nature of the phenomena, one has to make sure of a potential power dissipation of such a device. We consider that approximately  $\sim 50\%$  of the laser power is absorbed in the two ITO layers, which then heats the local volume of the LC. For a laser power of 90 mW and the illumination time of 10 ms we estimate from Figure 5 that a circular volume with diameter of  $\sim 30$   $\mu\text{m}$  shall be heated on average up to  $\sim 65^\circ\text{C}$  (half width at half maximum temperature). Therefore an energy of  $\sim 450$   $\mu\text{J}$  has to be used to heat a 30  $\mu\text{m}$  diameter ‘pixel’ from the room temperature up to  $\sim 65^\circ\text{C}$ . At a frame rate of 30Hz, this requires an average driving power of 13.5 mW per 30  $\mu\text{m}$  diameter pixel. This corresponds to a surface power dissipation of 19  $\mu\text{W}/\mu\text{m}^2$ , which for a screen of 1 m requires an operational power of the order of 19 MW! It is quite clear that any LC device operating on thermal tuning of the birefringence is not practical because of its huge power consumption.

#### Disclosure statement

No potential conflict of interest was reported by the authors.

#### References

- [1] Ashkin A. Acceleration and trapping of particles by radiation pressure. *Phys Rev Lett.* 1970;24:156–159.

- [2] Yada M, Yamamoto J, Yokoyama H. Direct observation of anisotropic interparticle forces in nematic colloids with optical tweezers. *Phys Rev Lett.* 2004;92:185501.
- [3] Muševič I, Škarabot M, Babič D, et al. Laser trapping of small colloidal particles in a nematic liquid crystal: clouds and ghosts. *Phys Rev Lett.* 2004;93:187801.
- [4] Noel CM, Bossis G, Chaze AM, et al. Measurement of elastic forces between two colloidal particles in a nematic liquid crystal. *Phys Rev Lett.* 2006;96:217801.
- [5] Smalyukh I, Kachynski AV, Kuzmin AN, et al. Laser trapping in anisotropic fluids and polarization-controlled particle dynamics. *Proc Natl Acad Sci.* 2006;103:1804818053.
- [6] Škarabot M, Ravnik M, Babič D, et al. Laser trapping of low refractive index colloids in a nematic liquid crystal. *Phys Rev E.* 2006;73:021705.
- [7] Muševič I, Škarabot M, Tkalec U, et al. Two-dimensional nematic colloidal crystals self-assembled by topological defects. *Science.* 2006;313:954–957.
- [8] Smalyukh I, Kaputa DS, Kachynski AV, et al. Optical trapping of director structures and defects in liquid crystals using laser tweezers. *Opt Exp.* 2007;15:4359.
- [9] Takahashi K, Ichikawa M, Kimura Y. Force between colloidal particles in a nematic liquid crystals studied by optical tweezers. *Phys Rev E.* 2008;77:020703.
- [10] Tkalec U, Ravnik M, Čopar S, et al. Reconfigurable knots and links in chiral nematic colloids. *Science.* 2011;333:62.
- [11] Jampani VSR, Škarabot M, Ravnik M, et al. Colloidal entanglement in highly twisted chiral nematic colloids: twisted loops, Hopf links and trefoil knots. *Phys Rev E.* 2011;84:031.
- [12] Lucchetti L, Criante L, Bracalente F, et al. Optical trapping induced by reorientational nonlocal effects in nematic liquid crystals. *Phys Rev E.* 2011;84:021702.
- [13] Škarabot M, Lokar Ž, Muševič I. Transport of particles by a thermally induced gradient of the order parameter in nematic liquid crystals. *Phys Rev E.* 2013;87:062501.
- [14] Francescangeli O, Slussarenko S, Simoni F, et al. Light-induced surface sliding of the nematic director in liquid crystals. *Phys Rev Lett.* 1999;82:1855–1858.
- [15] Khoo IC, Slussarenko S, Guenther BD, et al. Optically induced space-charge fields, dc voltage, and extraordinarily large nonlinearity in dye-doped nematic liquid crystals. *Opt Lett.* 1998;23:253–255.
- [16] Simoni F, Lucchetti L. Colossal nonlinear optical response of liquid crystals. *J Mol Liq.* 2018;267:67–72.
- [17] Iljin A. Light-induced order modification – the way to speed up. *J Mol Liq.* 2018;267:38–44.
- [18] Huang TC, Chen YY, Chu CC, et al. Optothermal switching of cholesteric liquid crystals: A study of azobenzene derivatives and laser wavelengths. *Materials.* 2015;8(9):6071–6084.
- [19] Oh SW, Kim SH, Baek JM, et al. Optical and thermal switching of liquid crystals for self-shading windows. *Adv Sustainable Syst.* 2018;2:1700164.
- [20] Mirri G, Škarabot M, Muševič I. In situ laser-imprinted surface realignment of a nematic liquid crystal. *Soft Matter.* 2015;11:3347–3353.
- [21] Jagemalm P, Herman DS, Komitov L, et al. Opto-thermal reorientation of nematics with two-fold degenerate alignment. *Liq Cryst.* 1998;24:335–340.
- [22] Chuang I, Durrer R, Turok N, et al. Cosmology in the laboratory: defect dynamics in liquid crystals. *Science.* 1991;251:1336–1342.
- [23] Bowick MJ, Chandar L, Schiff EA, et al. The cosmological Kibble mechanism in the laboratory: string formation in liquid crystals. *Science.* 1994;263:943–945.
- [24] Ryzhkova A, Jagodič U, Muševič I. Nanosecond incoherent light source for fast and low light microscopy. Submitted.
- [25] Scharf T. Polarized light in liquid crystals and polymers. New Jersey, USA: Wiley; 2007. p. 401.